Volume A 101 · Number 1 · October 2010

Applied Physics A
Materials Science & Processing

Special Issue: "Laser Ablation: Fundamentals"

Guest Editors: B. Luk'yanchuk, A. Vertes

continued on last cover page

Springer

Appl Phys A (2010) 101: 121–126
DOI 10.1007/s00339-010-5781-2

Applied Physics A
Materials Science & Processing

Ablation and analysis of small cell populations and single cells by consecutive laser pulses

Bindesh Shrestha · Peter Nemes · Akos Vertes

Received: 22 November 2009 / Accepted: 27 April 2010 / Published online: 3 June 2010

Abstract Laser ablation of single cells through a sharpened optical fiber is used for the detection of metabolites by laser ablation electrospray ionization (LAESI) mass spectrometry (MS). Ablation of the same *Allium cepa* epidermal cell by consecutive pulses indicates the rupture of the cell wall by the second shot. Intracellular sucrose heterogeneity is detected by subsequent laser pulses pointing to rupturing the vacuolar membrane by the third exposure. Ion production by bursts of laser pulses shows that the drying of ruptured *A. cepa* cells occurs in ∼50 s at low pulse rates (10 pulses/s bursts) and significantly faster at high pulse rates (100 pulses/s bursts). These results point to the competing role of cytoplasm ejection and evaporative drying in diminishing the LAESI-MS signal in ∼50 s or 100 laser pulses, whichever occurs first.

1 Introduction

Laser ablation of single cells or small cell populations has been applied to microsurgical modification of cell lineage in *Caenorhabditis elegans* and *Arabidopsis thaliana* [1, 2], to controlling the spatial orientation and the growth of cells [3], to laser-assisted cell direct writing [4, 5], etc. Shorter laser pulses, lasting for femtoseconds, have been used to ablate cell organelles, such as mitochondria, inside a live cell without affecting other neighboring organelles or the viability of the cell [6, 7].

Paper presented at the 10th International Conference on Laser Ablation, 2009, Singapore.

B. Shrestha · P. Nemes · A. Vertes (✉)
Department of Chemistry, George Washington University,
725 21st Street, NW, Washington, DC 20052, USA
e-mail: vertes@gwu.edu
Fax: +1-202-9945873

The ions produced by laser ablation can be detected by mass spectrometry for chemical analysis of single cells. Matrix-assisted laser desorption-ionization (MALDI) mass spectrometry (MS) was successfully utilized for peptide analysis in single cells [8] and for the analysis of biochemicals in cells extracted by laser capture microdissection [9, 10]. Ultraviolet MALDI, however, requires the introduction of an organic matrix in large excess and is most commonly practiced in vacuum environment. Laser ablation sampling of cells for chemical analysis at atmospheric pressure and without the introduction of exogenous materials is attractive because of the reduced perturbation of the biological specimen.

Most biological tissues and cells contain a significant amount of water. The strong absorption band of water at ∼2.94 μm wavelength, due to the OH vibrations, efficiently couples the mid-IR laser pulse energy into such targets. Shori et al. showed that the absorption of mid-IR laser pulses became a nonlinear process at the elevated fluences required for ablation [11]. According to the fast imaging observations of Apitz and Vogel, the ablation of water proceeds in three partially overlapping stages [12]. In the initial few hundred nanoseconds after irradiation, surface evaporation and phase explosion take place producing a dense plume that rapidly expands [13, 14]. In the presence of atmospheric pressure, the expansion slows down, stops, and the plume collapses back onto the sample surface. As a consequence, pressure builds up in the target that ultimately relaxes through the ejection of particulate matter for up to hundreds of microseconds. Similarly, soft tissues with high water content undergo recoil-induced secondary material expulsion, which results in an increased efficiency of ablation.

Mid-IR laser ablation of water-rich samples at atmospheric pressure produces mostly neutrals and particulate matter and only a small fraction of ions. The direct sampling of

these ions has been utilized to analyze plant and animal tissues as well as human bodily fluids [15–17]. In the laser ablation electrospray ionization (LAESI) MS, the nonionized portion of the ablation plume is converted to ions by an electrospray source. The LAESI-MS has been utilized to analyze biochemicals in various plant organs, human bodily fluids, and the electric organ of torpedo fish [18–20]. Recently, single plant and animal cells were analyzed by LAESI-MS by producing laser ablation at the cellular scale [21]. This was achieved by delivering and focusing the laser light to the target through a sharpened optical fiber, an approach similar to scanning near-field optical microscopy [22].

Ablation of individual cells requires the rupture of the cell wall or the cell membrane. Once the cytoplasm is exposed, consecutive laser pulses induce its ejection until depletion in the ablated cell. Thus the onset of ablation and the shot-by-shot course of single cell analysis are different from the response of unconfined liquid surfaces. In this contribution we compare the laser ablation of cells using conventional and sharpened optical-fiber-based focusing, as well as the ablation of aqueous solutions and individual cells using the LAESI process for the ionization of the ejected material.

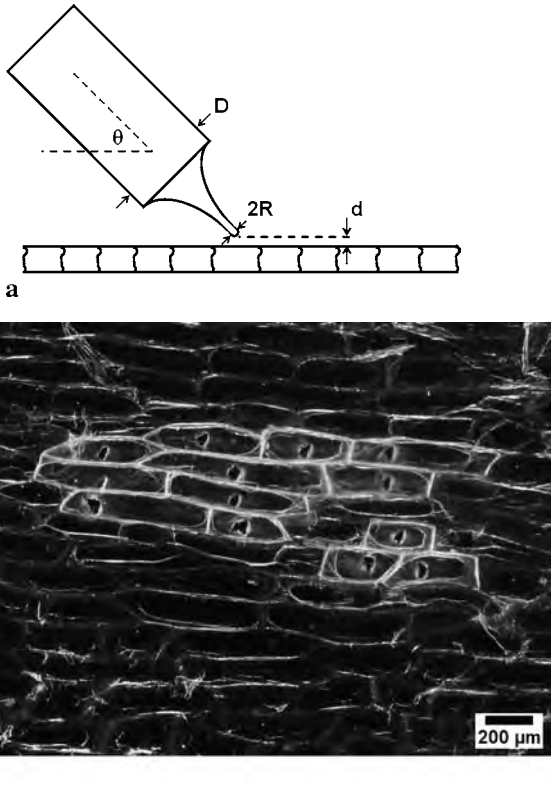

Fig. 1 **(a)** Schematic representation of the laser ablation geometry for energy deposition through a sharpened optical fiber. Parameters D, R, θ, and d stand for the optical fiber core diameter, the etched tip radius of curvature, the angle of inclination, and the distance from the tissue surface, respectively. **(b)** Ablation marks on single adjacent *A. cepa* cells

2 Experimental

The experimental setup used in the presented study for the ablation and to obtain the LAESI mass spectra have been described in detail elsewhere [18, 21]. The relevant aspects of these systems are briefly discussed later in the article.

2.1 Mid-infrared laser and optics

Mid-IR laser pulses at 2.94 µm wavelength with 5-ns pulse length were generated by a diode-pumped Nd:YAG laser driven optical parametric oscillator (Opolette 100, Opotek Inc., Carlsbad, CA). Maximum repetition rate of the laser was 100 Hz. Individual laser pulses were selected by a high-performance optical shutter (SR470, Stanford Research Systems, Inc., Sunnyvale, CA) and the laser beam was steered by gold-coated mirrors (PF10-03-M01, Thorlabs, Newton, NJ).

For the ablation of tissues using conventional focusing, circular ablation spots of 250–300 µm in diameter were produced by focusing the laser beam by either a single 75-mm focal length plano-convex antireflection-coated ZnSe lens (>95% transmission at 3 µm wavelength) or by a 150-mm focal length plano-convex CaF_2 lens (>90% transmission at 3 µm wavelength) (Infrared Optical Products, Farmingdale, NY). In the single cell studies, the mid-IR laser light was delivered through a sharpened germanium oxide (GeO_2) based optical fiber with $D = 450$ µm core diameter (HP Fiber, Infrared Fiber Systems, Inc., Silver Spring, MD). A 50-mm focal length plano-convex CaF_2 lens (Infrared Optical Products, Farmingdale, NY) was used to focus the laser beam onto one end of the fiber. The diameter of the illuminated area was ~75% of that of the fiber core to prevent damaging the cladding and to achieve efficient coupling [23].

The other end of the optical fiber was chemically etched in 1% HNO_3 solution to achieve a tip with $R = 15$ to 50 µm radius of curvature for the efficient delivery of laser energy to individual cells. The tip with 15-µm radius of curvature was produced by vertically lowering the fiber end ~300 µm deep into the etchant from the point of the initial contact with the acid solution. Following 15 min of etching, the produced tip spontaneously detached from the etchant surface. Then the tip was rinsed with deionized water to remove the residues of the etchant. To obtain the tip with the larger 50-µm radius, the fiber end was immersed ~1.5 mm into the acid solution. After 20 min of treatment, the etched tip was removed from the acid solution before the tip spontaneously detached from the surface.

Close to the etched end, the fiber was held by a micromanipulator (MN-151, Narishige, Tokyo, Japan) at an inclination angle, θ, of 45° and its tip was monitored by a long-distance video microscope (InFocus Model KC, Infin-

ity, Boulder CO, USA) with an infinity-corrected 5× objective lens (M Plan Apo 5×, Mitutoyo Co., Kanagawa, Japan). The distance between the fiber tip and the sample surface, d, was visualized by a CCD camera (Marlin F131, Allied Vision Technologies, Stadtroda, Germany). A schematic of the ablation geometry is shown in Fig. 1a.

2.2 LAESI source and mass spectrometer

The particulate matter ejected by the ablation was ionized by a homebuilt electrospray source. A syringe pump (Harvard Apparatus, Holliston, MA, USA) supplied an aqueous solution containing 50% methanol and 0.1% (v/v) acetic acid at 200 nL/min flow rate through a tapered tip stainless steel emitter (i.d. 50 µm, New Objective, Woburn, MA, USA). Electrospray was generated by applying stable high voltage between +2.7 and +2.9 kV to the metal emitter using a regulated power supply (Stanford Research Systems, Sunnyvale, CA, USA). The sample was placed on a microscope slide mounted 10–15 mm below the emitter. An orthogonal acceleration time-of-flight mass spectrometer (Q-TOF Premier, Waters Co., MA) with a mass resolution of 8000 (FWHM) collected and analyzed the ions produced by the LAESI source.

2.3 Materials and biological samples

Glucose (Sigma, St. Louis, MO), acetic acid (Fluka, Munich, Germany), methanol (Sigma, St. Louis, MO), and HPLC grade water (Acros Organics, Geel, Belgium) utilized in the study were used without further purification. *Allium cepa* and *Narcissus pseudonarcissus* were obtained locally, from Washington, DC, and Reston, VA, respectively. Prior to the analysis, the plant tissues were excised and directly mounted on glass microscope slides.

3 Results and discussion

3.1 Ablation using conventional focusing or sharpened fiber

Laser ablation for chemical analysis is mostly performed using conventional focusing of the light that relies on lenses and mirrors. An alternative approach demonstrated for single cell ablation, which can provide tighter focusing and allows flexibility in the sample ablation geometry, is the delivery of the laser pulse energy through an etched optical fiber tip.

Initially we compared the utility of these two focusing techniques for LAESI-MS analysis of tissues and cells. Figures 2a and 2b show LAESI mass spectra obtained by ablating small cell populations of *N. pseudonarcissus* epidermal cells using a 150-mm focal length plano-convex CaF_2 lens (10 to 20 cells) and an etched fiber tip with $R = 50$ µm radius of curvature held at $d = \sim 30$ µm from the surface (2 to 5 cells), respectively. Although the ablation through the lens affected more cells, no significant difference was observed in the mass spectra. Many of these ions had been

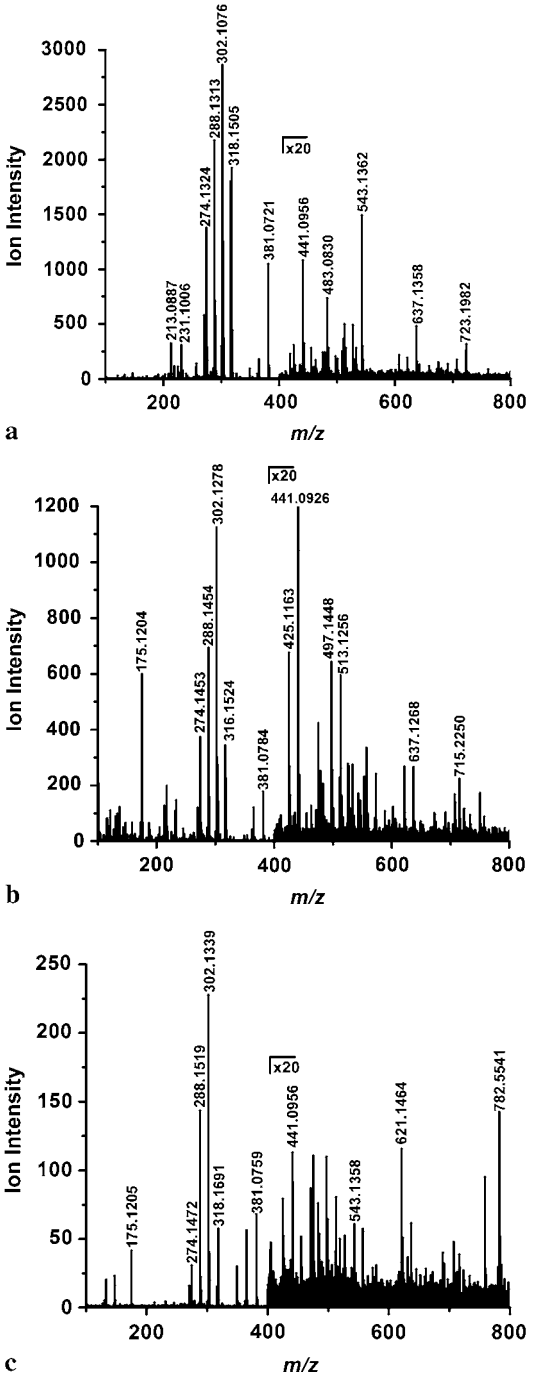

Fig. 2 Comparison of LAESI mass spectra collected from the epidermis of *N. pseudonarcissus* upon **(a)** conventional focusing with a CaF_2 lens and **(b)** and **(c)** with an etched GeO_2-based fiber tip. Panels **(a)** and **(b)** present mass spectra from small cell populations, whereas panel **(c)** shows the spectrum from a single epidermal cell

identified as metabolites known to be present in these tissues [21]. These results also show that in a LAESI experiment there is minimal loss of mass spectral signal due to the interference between the fiber tip and the ablation plume. This was somewhat surprising, as the fiber tip formed an obstruction for the expansion of the plume raising the possibility of plume deflection and the deposition of ablation products on the fiber. Therefore, we inspected the fiber tip with an optical microscope to check its integrity and the presence of contamination. After performing multiple ablations, the fiber tip appeared unchanged with no visible sign of contamination present.

In order to ablate individual cells, sharper fiber tips were produced by increasing the chemical etching time. A single cell ablation was achieved when a fiber tip with $R = 15$ μm radius of curvature was held at $d = \sim 30$ μm distance from the tissue surface and was positioned at the center of the exposed cell wall. Ablations under these conditions ruptured the cell wall and produced openings with an average diameter of 45 μm (see Fig. 1b).

As LAESI mass spectra were detected after these ablations, we infer that cytoplasm was ejected through these openings. Figure 2c presents such a mass spectrum produced by ~100 ablations at 100 Hz repetition rate from a single *N. pseudonarcissus* cell. Many ions detected in the mass spectra for cell populations, shown in Figs. 2a and 2b, were also found in the mass spectra for single cells (see, for example, Fig. 2c), although the ion counts were approximately an order of magnitude lower. The reduced ion intensity was a consequence of the smaller ablated volume. Differences between the average metabolic makeup of a cell population and an individual cell can be attributed to variations in internal and environmental factors.

3.2 LAESI-MS signal as a function of repetition rate

As the ion signal in the mass spectra corresponded to multiple laser pulses, we tested whether the repetition rate, i.e., the time that elapsed between the individual shots, affected the ion production. Such an effect would be indicative of interactions between consecutive ablations. To eliminate the influence of natural variations in biological samples, in these experiments 5.6-mM glucose solution was used as a target. Laser pulse repetition rates of 10, 25, 50, and 100 Hz were compared looking at the sodiated glucose signal at m/z 203 for 1, 5, and 10 shots selected by the programmable optical shutter.

Figure 3 shows the sodiated glucose peak area as a function of the number of delivered laser pulses for 10 and 100 Hz repetition rates or 100 and 10 ms between laser pulses. The readings for 25 and 50 Hz rates were very similar. From the data in Fig. 3 it is clear that reducing the time

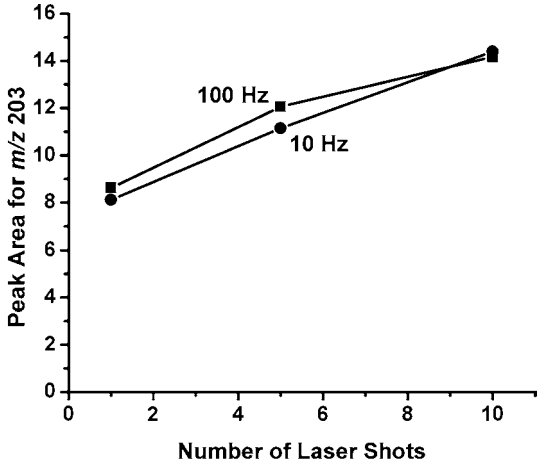

Fig. 3 LAESI-MS ion intensity for sodiated glucose (m/z 203) from aqueous solution, as a function of the number of laser pulses during a 1-s scan for 100 (10 Hz) and 10 ms (100 Hz) times elapsed between shots

between laser pulses to 10 ms does not affect ion production. Thus, in terms of particulate ejection, laser pulses that are at least 10 ms apart can be viewed as independent.

Figure 3 also indicates that an increase in the number of delivered pulses results in a linear growth in ion production. The gain from multiple pulses, however, is not additive, i.e., delivering ten laser shots does not produce ten times more ions. In light of the apparent independence of the ablation events, this observation is especially peculiar. The lack of additivity can be explained based on the interaction between the laser ablation plume and the electrospray plume. Although the additional laser pulses increase ion production through the enhanced supply of particulate matter, the ablation plume also perturbs the electrospray thereby moderating the gain in the ions collected by the mass spectrometer.

3.3 Single cell ablation by consecutive single pulses

Single-cell ablation experiments on *A. cepa* epidermal cells indicated an important difference from the ablation of free solution surfaces described in the previous section. For cells, in most cases, the first laser pulse did not produce an ion signal, because the cell wall did not rupture. Usually, the cell wall broke during the second laser pulse resulting in LAESI ion production for a few consecutive shots. Representative spectra from a sequence of four laser pulses, delivered 10 s apart and impinging on the on same *A. cepa* epidermal cell, are presented in Fig. 4a.

The lack of signal upon the first laser pulse is followed by a LAESI-MS spectrum with high signal-to-noise ratio. The mass spectra recorded for the second and the fourth laser pulses indicated similar ion composition and abundances. The third pulse often produced higher abundances for certain ions, for example, for the potassiated sucrose species

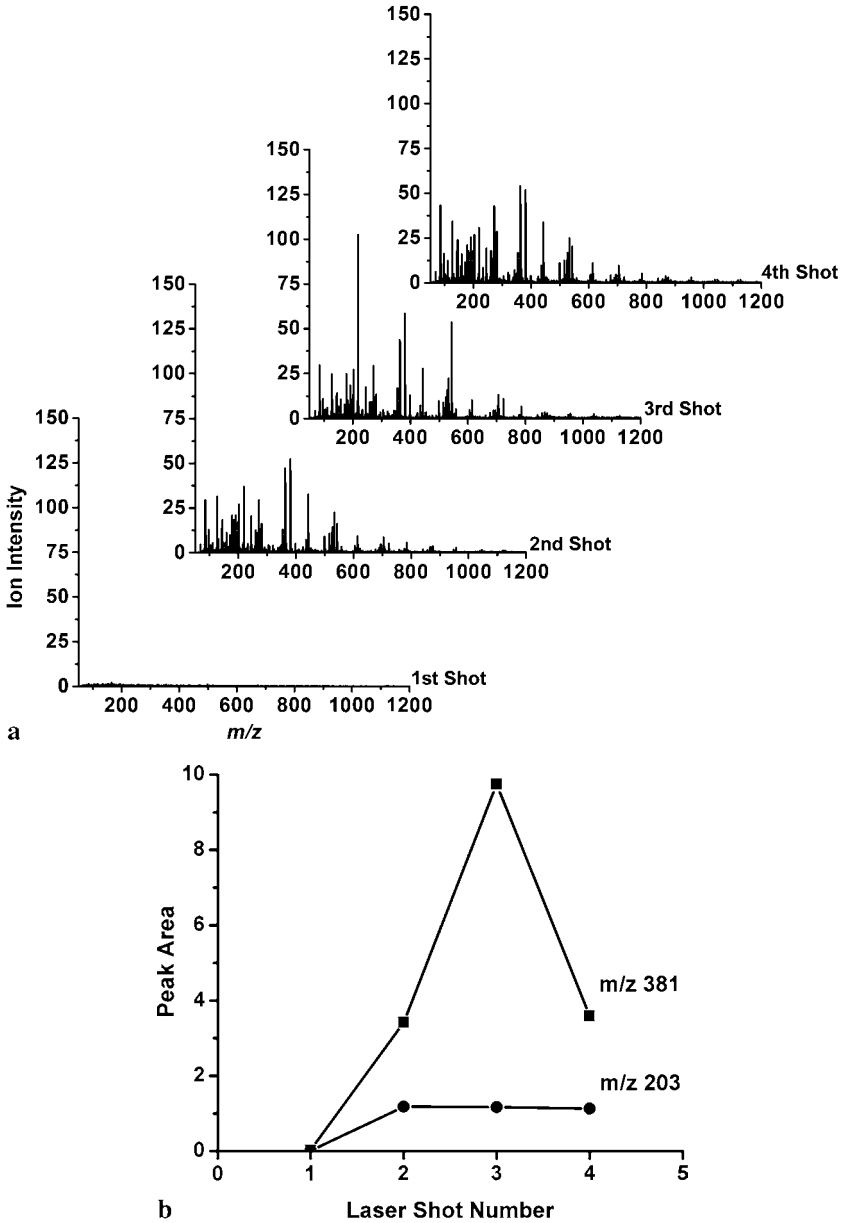

Fig. 4 **(a)** LAESI mass spectra from single *A. cepa* cell produced by consecutive laser pulses. The first laser shot did not produce noticeable LAESI-MS signal, whereas the second to fourth pulses produced spectra with high signal-to-noise ratio. LAESI mass spectra recorded after the fourth pulse did not yield signal. **(b)** LAESI-MS ion intensity for sodiated glucose (m/z 203) and potassiated sucrose (m/z 381) from a single *A. cepa* cell produced by consecutive laser pulses

with m/z 381. This observation is depicted in Fig. 4b that compares the shot-by-shot peak areas for the m/z 381 and 203 (sodiated glucose/fructose) ions. Comparing the behavior of the two ions seems to indicate that the spiking of the sucrose related signal is due to the internal inhomogeneity of the cell. Indeed, it is known that vacuoles, organelles that typically occupy from 30 up to 80% of the cell volume in plants, can store significant amounts of sucrose [24, 25]. It is perceivable that the third laser pulse induced the rupture of the vacuolar membrane and released/ablated the content of the vacuole. If this scenario is, indeed, valid these experiments point to the possibility of analyzing cell organelle metabolites using the described LAESI-MS based approach.

Typically, after the fourth or the fifth laser pulse no appreciable ion counts were recorded. The lack of signal in these cases can be attributed to the removal of all the cytoplasm by the previous 4–5 pulses or to the dehydration of the exposed cell interior due to evaporation of its water content in 40–50 s. To assess the relative importance of cytoplasm removal by the laser pulses and cell drying, we conducted experiments with bursts of 10 and 100 laser pulses in 1 s separated by 10 s intermissions. We found that delivering 10 pulses/s to a similar *A. cepa* cell produced signal for 40–50 pulses and 40–50 s. These two observations pointed to the dominant role of evaporative drying in these cases. Increasing the repetition rate to 100 Hz and delivering 100 pulses/s in a burst followed by a 10 s intermission indicated the pres-

ence of signal for 100 pulses and the lack of signal in the second burst. In this particular case, the combined effect of cytoplasm removal in the first burst and evaporative drying during the first 10 s intermission could explain our observations. Based on the role of evaporative drying established by these experiments, controlling the humidity of the environment is needed to improve signal stability and reproducibility. The applied 2.94-μm mid-IR light, however, is strongly attenuated by high humidity. Performing these experiments in an environmental chamber is facilitated by the fiber-optics-based laser pulse delivery because the mid-IR light only has to travel a short distance (∼30 μm) in the elevated humidity environment.

Acknowledgements The presented work was supported by the National Science Foundation (grant No. 0719232). The opinions, findings, conclusions, or recommendations in the material are those of the authors and do not necessarily reflect the views of the supporting organizations. The germanium-oxide-based optical fibers used in this study were kindly donated by Infrared Fiber Systems, Inc., Silver Spring, MD.

References

1. J. Kimble, Dev. Biol. **87**, 286 (1981)
2. C. van den Berg, V. Willemsen, W. Hage, P. Weisbeek, B. Scheres, Nature **378**, 62 (1995)
3. P. Li, U. Bakowsky, F. Yu, C. Loehbach, F. Muecklich, C. Lehr, IEEE Trans. Nanobiosci. **2**, 138 (2003)
4. B.R. Ringeisen, D.B. Chrisey, A. Pique, H.D. Young, R. Modi, M. Bucaro, J. Jones-Meehan, B.J. Spargo, Biomaterials **23**, 161 (2002)
5. G. Li, Y. Huang, J. Manuf. Sci. Eng. **131**, 051013 (2009)
6. M.F. Yanik, H. Cinar, H.N. Cinar, A.D. Chisholm, Y.S. Jin, A. Ben-Yakar, Nature **432**, 822 (2004)
7. N. Shen, D. Datta, C. Schaffer, P. LeDuc, D. Ingber, E. Mazur, Mech. Chem. Biosyst. **2**, 17 (2005)
8. L. Li, R. Garden, J. Sweedler, Trends Biotechnol. **18**, 151 (2000)
9. M.R. EmmertBuck, R.F. Bonner, P.D. Smith, R.F. Chuaqui, Z.P. Zhuang, S.R. Goldstein, R.A. Weiss, L.A. Liotta, Science **274**, 998 (1996)
10. B. Xu, R. Caprioli, M. Sanders, R. Jensen, J. Am. Soc. Mass Spectrom. **13**, 1292 (2002)
11. R.K. Shori, A.A. Walston, O.M. Stafsudd, D. Fried, J.T. Walsh Jr., IEEE J. Sel. Top. Quantum Electron. **7**, 959 (2001)
12. I. Apitz, A. Vogel, Appl. Phys. A Mater. Sci. Process. **81**, 329 (2005)
13. Z. Chen, A. Bogaerts, A. Vertes, Appl. Phys. Lett. **89**, 041503 (2006)
14. Z.Y. Chen, A. Vertes, Phys. Rev. E **77**, 036316 (2008)
15. Y. Li, B. Shrestha, A. Vertes, Anal. Chem. **79**, 523 (2007)
16. Y. Li, B. Shrestha, A. Vertes, Anal. Chem. **80**, 407 (2008)
17. B. Shrestha, Y. Li, A. Vertes, Metabolomics **4**, 297 (2008)
18. P. Nemes, A. Vertes, Anal. Chem. **79**, 8098 (2007)
19. P. Nemes, A.A. Barton, Y. Li, A. Vertes, Anal. Chem. **80**, 4575 (2008)
20. P. Sripadi, J. Nazarian, Y. Hathout, E. Hoffman, A. Vertes, Metabolomics **5**, 263 (2009)
21. B. Shrestha, A. Vertes, Anal. Chem. **81**, 8265 (2009)
22. R. Stockle, P. Setz, V. Deckert, T. Lippert, A. Wokaun, R. Zenobi, Anal. Chem. **73**, 1399 (2001)
23. R.M. Verdaasdonk, C. Borst, in *Optical-Thermal Response of Laser-Irradiated Tissue*, ed. by A.J. Welch, M.J.C.V. Gemert (Plenum, New York, 1995), p. 619
24. A. Endler, S. Meyer, S. Schelbert, T. Schneider, W. Weschke, S.W. Peters, F. Keller, S. Baginsky, E. Martinoia, U.G. Schmidt, Plant Physiol. **141**, 196 (2006)
25. A.K. Grennan, J. Gragg, Plant Physiol. **150**, 1109 (2009)